JOC Article

N7-Guanine as a C^+ Mimic in Hairpin *aeg*/*aep*PNA-DNA Triplex: Probing Binding Selectivity by UV-T_m and Kinetics by Fluorescence-Based Strand-Invasion Assay

Moneesha D'Costa, Vaijayanti A. Kumar,* and Krishna N. Ganesh

Division of Organic Chemistry (Synthesis), National Chemical Laboratory, Pune, 411008, Maharashtra, India

vkumar@dna.ncl.res.in

Received January 15, 2003

N7-substituted guanine (N7G) has been introduced into aminoethylglycyl bisPNA (**7**) as a C^+ mimic to achieve pH-independent triplex formation with complementary DNA sequences. The introduction of chiral, cationic aminoethylprolyl units with C^+ and C^+ mimic N7G in the backbone of bisPNAs (**8**, **9**) influenced the recognition of complementary DNA in an orientation-selective manner. A simple fluorescence assay is developed to examine the process of strand invasion of target DNA duplex by these modified bisPNAs and comparative results of the study employing triplex forming polypyrimidine (C/T) (**6**, **8**) and purine-pyrimidine (N7G/T) mixmer-bisPNAs (**7**, **9**) are presented.

Introduction

Peptide nucleic acids (PNAs) are neutral, achiral DNA mimics that bind to complementary DNA/RNA sequences with high affinity and sequence specificity.[1] Homopyrimidine PNA sequences form PNA_2:DNA triplexes in which PNA (parallel or antiparallel) is involved in either Watson−Crick (WC) or Hoogsteen (HG) hydrogen bonding modes with the central polypurine DNA strand (Figure 1a).[2] In such PNA_2:DNA triplexes, the DNA strand is engaged in simultaneous binding to two PNA strands and ambiguity persists in establishing the specific correlation among parallel/antiparallel PNA strands with HG or WC binding mode with DNA.[2,3] In practice, this would lead to the formation of PNA_2:DNA triplexes with different combinations of various parallel/antiparallel strand orientations. The uncertainty in WC/HG PNA strand orientation with respect to DNA of such mixed PNA_2:DNA complexes can be partially overcome by conjugating the two PNA strands with a linker to construct a bisPNA hairpin that can form only two triplexes with a 1:1 (PNA:DNA) composition.[4] We envisaged that introduction of a chiral identifier into one arm of the bisPNA may further help fix its orientation. We have recently reported[5] studies on aminoethylprolyl (*aep*) PNA, which is a chiral, positively charged PNA analogue of aminoethylglycyl (*aeg*) PNA. Oligothymine *aep*PNAs exhibited excellent binding properties with complementary DNA sequences.[5a] The mixmer PNAs with a chiral (2*S*,4*S*)-*aep*PNA unit that is configurationally homomorphous with DNA were found to induce orientational preferences during duplex formation with complementary DNA sequences.[5b] In this paper, we describe the potential of such a strategy by using mixed polypyrimidine bisPNA sequences containing *aep*PNA units at selected positions and their effects on directing the orientation-selectivity of DNA during triplex formation.[6]

In DNA triplexes, natural N9G binds in a reverse HG mode to a G:C base-pair in a purine motif, with the third strand in an antiparallel orientation[7] (Figure 1b). The pyrimidine motif requires N3-protonation of C and hence acidic conditions for stable triplex formation,[7] even in PNA:DNA triplexes.[8] N7G can replace protonated C (C^+) in the pyrimidine motif as its mimic (Figure 1c) and allows the formation of stable triplexes at neutral pH[9] in HG mode. In PNA_2:DNA triplexes, the two H-bond donor sites of the N7G as a C^+ mimic may recognize the G through HG mode in both parallel (Figure 1c) and antiparallel (Figure 1d) orientations, but may not recognize G in the WC binding mode (Figure 1e). Incorporation of N7G units in the PNA strand may thus stabilize triplexes only when engaged in the HG mode of binding unlike cytosine or "J" base—another C^+ mimic.[10] Incorporation of the N7G unit in PNA as a C^+ mimic in either

(1) (a) Nielsen, P. E. *Acc. Chem. Res.* **1999**, *32*, 624−630. (b) Ganesh, K. N.; Nielsen, P. E. *Curr. Org. Chem.* **2000**, *4*, 931−943.

(2) Egholm, M.; Christensen, L.; Dueholm, L. D.; Buchardt, O.; Coull, J.; Nielsen, P. E. *Nucleic Acids Res.* **1995**, *23*, 217−222.

(3) Parallel: N-terminal of PNA facing the 5′-end of DNA in the complex. Antiparallel: C-terminal of PNA facing the 5′-end of DNA.

(4) Griffith, M. C.; Risen, L. M.; Greig, M. J.; Lesnik, E. A.; Sprankle, K. G.; Griffey, R. H.; Kiely, J. S.; Freier, S. M. *J. Am. Chem. Soc.* **1995**, *117*, 831−832.

(5) (a) D'Costa, M.; Kumar, V. A.; Ganesh, K. N. *Org. Lett.* **1999**, *1*, 1513−1516. (b) D'Costa, M.; Kumar, V. A.; Ganesh, K. N. *Org. Lett.* **2001**, *3*, 1281−1284. (c) Kumar, V. A. *Eur. J. Org. Chem.* **2002**, 2021−2032.

(6) A very preliminary report presented as a poster at the XIVth IRT Symposium on Nucleosides and Nucleotides. Kumar, V. A.; D'Costa, M.; Ganesh, K. N. *Nucleosides Nucleotides Nucleic Acids* **2001**, *20*, 1187−1191.

(7) Beal, P. A.; Dervan, P. B. *Science* **1991**, *251*, 1360−1363.

(8) Egholm, M.; Buchardt, O.; Nielsen, P. E.; Berg, R. H. *J. Am. Chem. Soc.* **1992**, *114*, 1895−1897.

(9) (a) Brunar, H.; Dervan, P. B. *Nucleic Acids Res.* **1996**, *24*, 1987−1991. (b) Hunziker, J.; Priestley, E. S.; Brunar, H.; Dervan, P. B. *J. Am. Chem. Soc.* **1995**, *117*, 2661−2662.

(10) Kuhn, H.; Demidov, V. V.; Frank-Kamenetskii, M. D.; Nielsen, P. E. *Nucleic Acids Res.* **1998**, *26*, 582−587.

10.1021/jo034048h CCC: $25.00
Published on Web 05/06/2003

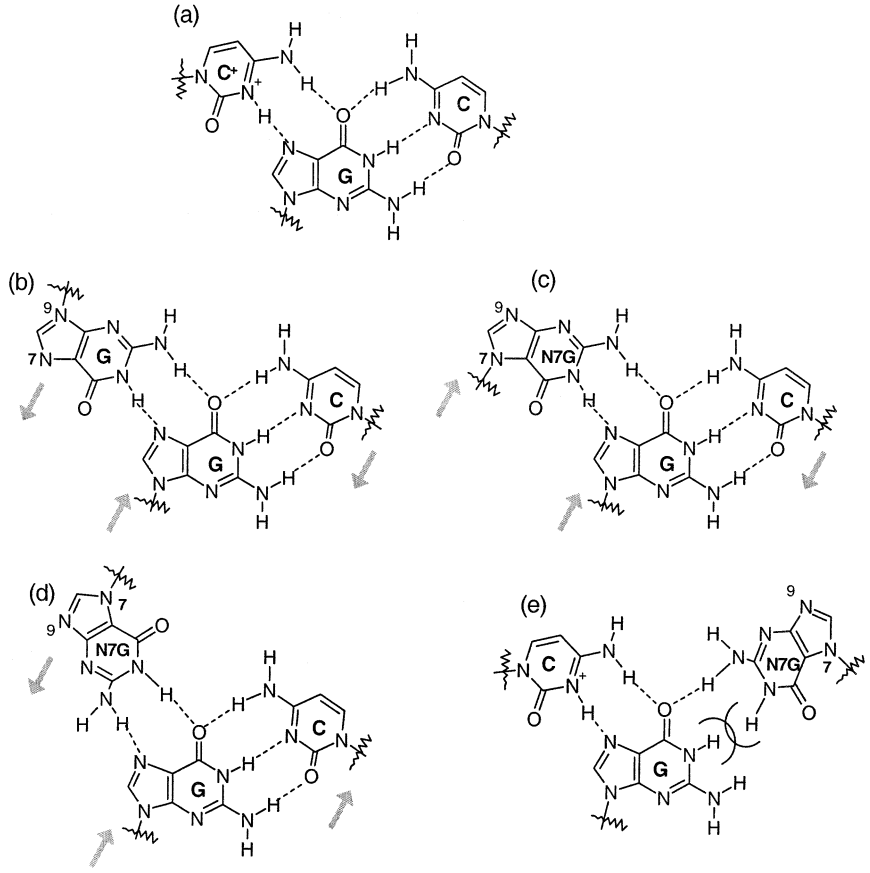

FIGURE 1. Hydrogen bonding schemes: (a) $C^{+}_{p/ap}$∗G:$C_{p/ap}$, (b) G_{ap}∗G:C_{ap}, (c) $N7G_{p}$∗G:C_{ap}, (d) $N7G_{ap}$∗G:C_{p}, and (e) C^{+}_{p}∗G:$N7G_{ap}$ [p = parallel; ap = antiparallel; ∗ indicates Hoogsteen H-bonding; : indicates WC H-bonding].

*aeg*PNA or *aep*PNA backbone is not yet known and this is the first such report.

We had earlier reported an easy fluorescence-based technique to study the kinetics of PNA:DNA duplex formation by the use of intrinsic fluorescence properties of 2-aminopurine.[11] We present here an easy and novel assay, based on the fluorescence properties of the commonly used intercalator, ethidium bromide.[12] This assay is shown to delineate the kinetics of strand invasion from the thermodynamic stability of the resulting bisPNA:DNA triplexes.

Synthesis of N7G *aeg*/*aep*-PNA. The PNA-N7G monomer synthons **2b** and **4b** and the *aep*PNA-C synthon **5b** were synthesized according to Scheme 1. N^2(^{i}Bu)-guanine was reacted with either *N*-Boc-aminoethyl-*N*-chloroacetyl glycinate **1**[13] or the *N*-Boc-aminoethyl-prolyl-4-*O*-mesylate **3**[5b] to obtain the corresponding N7-G PNA monomer esters (**2a** and **4a**) which were hydrolyzed to the acids **2b** and **4b**, respectively. The appropriately protected *aep*PNA-C monomer **5b** was prepared according to the reported procedure.[5b] These were incorporated into the PNA sequences **6**−**9** (Figure 2) by solid-phase synthesis, using the standard Boc-chemistry.[5] The PNA sequences **6**−**9** were designed to be hairpin bisPNAs comprising two polypyrimidine arms A and B linked by a pentamide fragment derived from alternating lysine and aminohexanoic acid moieties.[8] The PNA oligomers were deprotected-cleaved from the resin by TFMSA-TFA, purified by HPLC, and characterized by MALDI-TOF mass spectrometry. The N7G-containing oligomers were additionally treated with aqueous ammonia at 55 °C for 16 h to achieve complete removal of exocyclic amino group protection.

UV-T_m Studies on Hairpin PNA-DNA Triplexes. The oligodeoxynucleotides **10** and **11**, identical in sequence but reversed in 5′−3′ direction, were used to probe the parallel/antiparallel binding preferences, studied by UV melting experiments at pH 5.8 and 7.4. The control bisPNA **6** having *aeg*PNA-C units as X in arm A binds to either DNA **10** or DNA **11** with the same affinity (∼45 °C) at pH 7.4 (entry 1, Table 1). A higher T_m (∼52 °C) was seen at acidic pH as expected ($\Delta T_m \sim 7$ °C) due to cytosine N3 protonation. The protonation of cytosine could be in either arm A or arm B of bisPNA **6**, with the protonated form leading to HG and the nonprotonated form leading to WC modes of recognition with both orientations (Figure 1a). The PNA **6** thus does not distinguish between the two arms of PNA in terms of binding in the WC or HG mode. The replacement of *aeg*PNA-C as X in arm A by the C^+ mimic *aeg*PNA-N7G (PNA **7**) gave complexes of nearly similar stabilities

(11) Gangamani, B. P.; Kumar, V. A.; Ganesh, K. N. *Chem. Commun.* **1997**, 1913−1914

(12) During the preparation of this paper, a generalized and rapid high-throughput screening system was reported for determining relative DNA binding affinity or sequence selectivity of small peptides by the decrease in the fluorescence intensity of ethidium bromide: Woods, C. R.; Ishii, T.; Wu, B.; Bair, K. W.; Boger, D. L. *J. Am. Chem. Soc.* **2002**, *124*, 2148−2152.

(13) Meltzer, P. C.; Liang, A. Y.; Matsudaira, P. *J. Org. Chem.* **1995**, *60*, 4305.

SCHEME 1. Synthesis of PNA Monomer Synthons: *aeg*PNA-N7G (2b), *aep*PNA-N7G (4b), and *aep*PNA-C (5b)

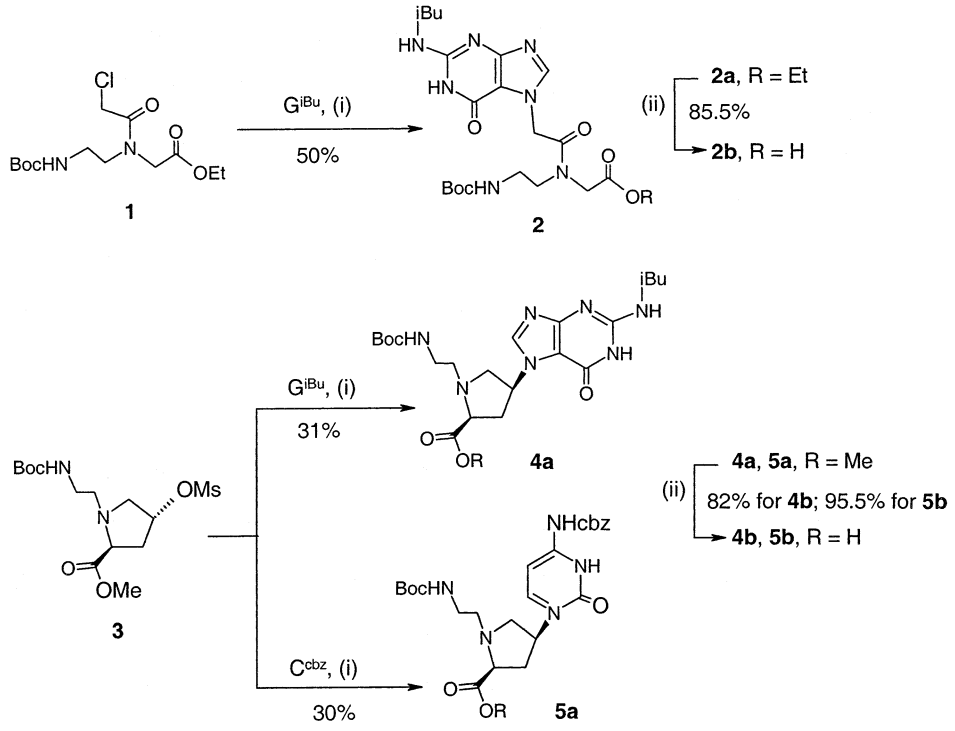

(i) K_2CO_3, 18-crown-6, DMF, (ii) NaOH, H_2O: MeOH (1:1)

(entry 2, Table 1) with the target DNA strands **10** and **11**. A marginal preference for antiparallel orientation of arm A as in complex **11**:**7** was observed over the parallel orientation of arm A as in complex **10**:**7** ($\Delta T_m = 2$ °C) at pH 7.4 (Figure 1d). Since the donor−acceptor H-bonding sites of N7G are not capable of recognizing G in the WC mode (Figure 1e), it is likely that arm A having N7G as X binds to DNA exclusively through the HG mode, but in either parallel (DNA **10**) or antiparallel (DNA **11**) orientation (Figure 1c,d).

In contrast to the achiral *aeg*PNA units, introduction of a chiral *aep*PNA-C unit as X in arm A in **8** leads to a stronger binding with DNA **11** ($T_m = 48$ °C) as compared to binding with DNA **10** ($T_m = 37.5$ °C) (entry 3, Table 1) at pH 7.4, suggesting a considerable bias ($\Delta T_m \sim 10$ °C) in the DNA orientation selectivity of binding. At acidic pH (5.8), the stability was enhanced in both cases, as expected from the protonation of N3 in C ($\Delta T_m \sim 10$ °C for DNA **10**; $\Delta T_m \sim 4$ °C for DNA **11**). However, binding of DNA **11** was significantly better than that of DNA **10**. It is possible that the cytosine N3 in *aeg*PNA-C and *aep*PNA-C units in the HG strand may have slightly different pK_a values. The possible protonation of the pyrrolidine ring nitrogen in the *aep*PNA at physiological pH[5] may also lower the pK_a of cytosine-N3 in *aep*PNA-C causing relatively less pronounced stabilizing effects at pH 5.8. Nevertheless, the observations in entry 3 indicate that the chiral *aep*PNA-C units in **8** stabilize the PNA:DNA (**8**:**11**) complex when present in the PNA strand (arm A) oriented antiparallel to the central DNA strand and recognition could be either in the HG or WC mode.[3] PNA **9** containing the chiral *aep*PNA-N7G unit as X in arm A exhibited a pronounced antiparallel preference to bind DNA **11** over DNA **10** at both acidic and neutral pH conditions (entry 4, Table 1, $\Delta T_m \sim 9$ °C) due to additive effects of the presence of the N7G nucleobase linked to a chiral *aep*PNA unit. Arm A in this case can bind only in the HG mode because of the presence of N7G units (Figure 1e), and thus PNA **9** binding to either DNA **10**/**11** does not exhibit pH-dependence (Figure 1d). The flexibility of the *aeg*PNA backbone in PNA **7** possibly allows the N7G nucleobase to bind to DNA **10** and DNA **11** with similar affinities, with a marginal preference for the antiparallel DNA **11** over parallel DNA **10**. On the other hand, the steric constraint and rigidity imposed by the pyrrolidine ring in *aep*PNA **9**, combined with its chirality, causes a significant bias in its binding to DNA **11** (antiparallel HG) over DNA **10** (parallel HG). Such a bias in binding of *aep*PNA to complementary parallel and antiparallel DNA sequences has been previously reported.[5b]

Fluorescence Assay for Strand Invasion. The bisPNA oligomers reported in this paper are appropriate to study the strand invasion properties by triplex formation when targeted toward duplex DNA. Ethidium bromide upon intercalation into a DNA duplex shows an increase in fluorescence intensity but is known not to interact with the PNA:DNA, PNA_2:DNA, or PNA:PNA complexes.[14] Strand invasion of the duplex DNA saturated with ethidium bromide by triplex-forming PNA oligomer should therefore cause a decrease in ethidium bromide fluorescence due to the disruption of DNA:DNA-ethidium bromide complex. The loss of ethidium bromide

(14) Wittung, P.; Kim, S. K.; Buchardt, O.; Nielsen, P.; Norden, B. *Nucleic Acids Res.* **1994**, *22*, 5371−5377.

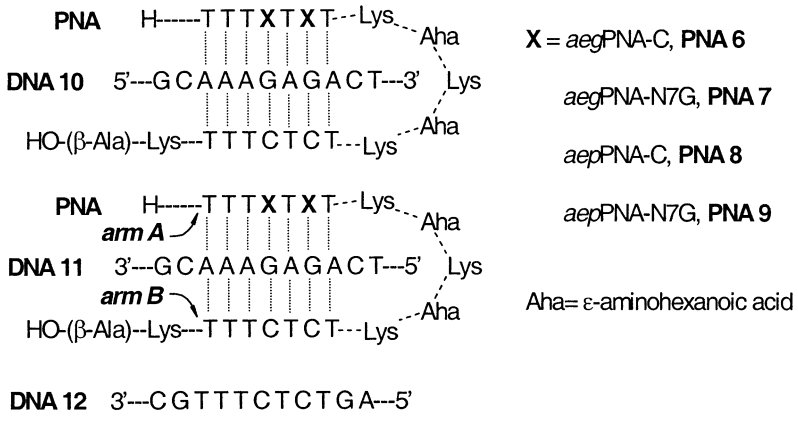

Arm A: DNA **10** (*p*); Arm B: DNA **10** (*ap*)
Arm A: DNA **11** (*ap*); Arm B: DNA **11** (*p*)

FIGURE 2. PNA oligomer sequences.

TABLE 1. UV Melting T_m of bisPNA-DNA Complexes[a]

entry	PNA	DNA **10**	DNA **11**
1	**6** *aeg*PNA-C	45 (52.7)	45 (52)
2	**7** *aeg*PNA-N7G	45 (47)	47 (45)
3	**8** *aep*PNA-C	37.5 (47)	48 (52)
4	**9** *aep*PNA-N7G	42 (43)	51 (49)

[a] UV T_m data (°C) for PNA:DNA complexes with DNA **10** and **11**. Values in parentheses indicate T_m at pH 5.8. Experiments were performed in 10 mM sodium phosphate buffer, pH 7.4. T_m values are accurate to ±1 °C and were obtained from the peaks in the first derivative plots of percent hyperchromicity vs temperature. Each experiment was performed at least twice

fluorescence as a function of time upon addition of triplex-forming PNA oligomers may be used to study the kinetics of duplex strand invasion in this fluorescent intercalator displacement assay.

We studied the effects of nucleobase and backbone modifications of bisPNAs presented here on the kinetics of strand invasion of a complementary DNA duplex by ethidium bromide displacement assay. This study would permit delineation of the effects of a chiral, positively charged *aep*PNA backbone with respect to C^+ and C^+ mimic N7G units. The set of DNA and PNA oligomers for this study comprised DNA duplex **10**:**12** and PNA oligomers **6**, **7**, **9**, and **8** wherein the complexes of **10** with **6**, **7**, **9** (at pH 7.4), and **8** (at pH 5.8) exhibited almost similar UV-T_m values (Table 1, $\Delta T_m = \pm 2$ °C). The DNA duplex **10**:**12** was saturated with ethidium bromide and the kinetics of the strand invasion process was examined by monitoring the fluorescence emission decay at 590 nm ($\lambda_{ex.}$ 490 nm) as a function of time after individually adding the four PNAs **6**−**9** over 60 h. The emission intensity in each case decreased exponentially at different rates over 20 h and thereafter remained constant.

The Homopyrimidine(C/T) *aeg*/*aep*PNA 6/8. The addition of *aeg*PNA-C **6** to the duplex DNA **10**:**12** exhibited rapid loss of ethidium bromide fluorescence at pH 5.8 (Figure 3) within an hour. The kinetics of strand invasion though slightly slow at pH 7.4, the process was essentially complete with the total change in fluorescence emission intensity comparable to that at pH 5.8 in the first hour. The difference in kinetics arises from nonpro-

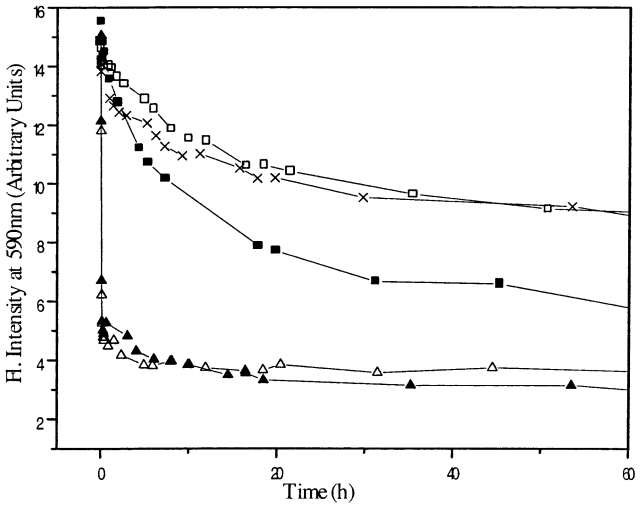

FIGURE 3. Ethidium bromide fluorescence as a function of time studied for the DNA duplex **10**:**12** after the addition of PNA **6** at pH 5.8 (△), PNA **6** at pH 7.4 (▲), PNA **8** at pH 5.8 (■), PNA **9** at pH 7.4 (□), and PNA **7** at pH 7.4 (×).

tonation of C in **6** at pH 7.4 and was not as prominent as reflected in its lower UV-T_m ($\Delta T_m = -8$ °C Table 1, entry 1, DNA **10**). The *aep*PNA-C **8** showed less decrease in emission intensity and a slower kinetics of ethidium bromide displacement as compared to the *aeg*PNA-C **6** even at pH 5.8. This could be a consequence of unfavorable stereochemical preferences imposed by the *aep* backbone in arm A of the PNA in parallel orientation with respect to DNA **10** or a relatively lower degree of protonation of cytosine N3 due to preferred pyrrolidine ring nitrogen protonation.

The Purine-Pyrimidine (N7G/T) PNA 7/9. The replacement of cytosine by a purine, N7G, a mimic of protonated cytosine at physiological pH, as in *aeg*PNA-N7G **7**, resulted in a lower decrease of the ethidium bromide fluorescence intensity and a plateau was reached only after 30 h (Figure 3). The slow kinetics of strand invasion in this case could be due to the presence of a purine unit in the pyrimidine-rich triplex-forming arm A of **7**, thereby affecting the hybridization competent

SCHEME 2. Strand Invasion of dsDNA by T/C- and T/N7G-Containing bisPNAs in the Presence of Ethidium Bromide

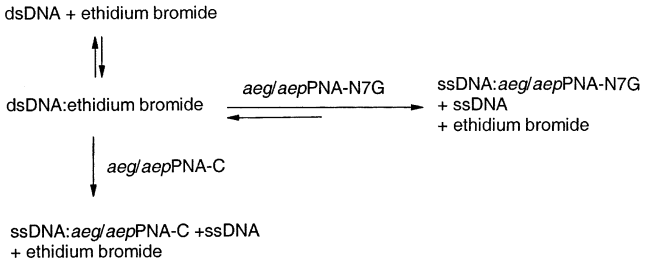

conformation of the *aeg*PNA backbone. The UV-T_m studies indicated almost equal efficiency of binding to the DNA **10** by both *aeg*PNA-C **6** and *aeg*PNA-N7G **7** at physiological pH (Table 1, entries 1 and 2, DNA **10**). Thermal melting, being under equilibrium conditions, does not reflect kinetic differences caused by the local perturbations of the backbone. The chiral *aep*PNA-N7G **9** showed very similar kinetics of strand invasion as achiral *aeg*PNA-N7G **7**, although the PNA:DNA complex **9**:**10** is less stable than **7**:**10** ($\Delta T_m = 3$ °C). The results overall suggested that the homopyrimidine bisPNAs **6** and **8** exhibit rapid kinetics of duplex strand invasion compared to N7G-PNAs **7** and **9**.

Interestingly, the strand invasion assay indicated significant differences in the final fluorescence intensities after duplex strand invasion by achiral *aeg*PNA-C and *aeg*PNA-N7G. The homopyrimidine *aeg/aep*PNA-C **6**, **8** displayed faster strand invasion kinetics. In contrast, with the purine-pyrimidine mixed PNA sequences **7** and **9** even after 60 h, the final fluorescence intensity was significant (~50%), suggesting incomplete strand displacement. The slower kinetics of strand invasion by PNA probably allows a reversible formation of dsDNA:EtBr complex when N7G is used as a C^+ mimic either with *aeg* or *aeg*/*aep* mixed backbone (Scheme 2). Strand invasion by hairpin homopyrimidine (T/C) *aeg*PNA is known to be an irreversible process[15] with maximum ethidium bromide displacement while the slow strand invasion by mixed purine-pyrimidine *aeg*/*aep*PNA is accompanied by reversible DNA duplex formation as seen by retention of ethidium bromide fluorescence.

The ethidium bromide displacement assay experiments presented here delineate the kinetics of the triplex formation by strand invasion and the thermodynamic stability of the resulting complexes as reflected in UV-T_m studies of novel *aeg*/*aep*-C/N7G bisPNAs with complementary DNA. Although the achiral *aeg*-N7G containing hairpin PNAs form stable complexes with single-stranded DNA (UV-T_m), these PNA oligomers show slower strand invasion kinetics seen in the ethidium bromide displacement assay. It should be pointed out that the fluorescence assay presented here is a simpler technique compared to the time-consuming footprinting and affinity cleavage techniques used previously to study the duplex invasion processes.[10]

In summary, the introduction of chiral *aep*PNA units in the backbone of triplex-forming PNA oligomers influenced the recognition of DNA in an orientation-selective manner as studied by UV-T_m. The triplex formation was pH-dependent when PNA-C units were used, while with PNA-N7G units, triplex formation was unaffected by pH variations. As expected for a neutral C^+ mimic, no differences in T_m were observed for both DNA **10** and DNA **11** as a function of pH. Among all triplexes, the most stable were observed for *aep*PNA-N7G at neutral pH with DNA **11**, where N7G binding to DNA was in a HG mode with preferred antiparallel third strand orientation. The ethidium bromide duplex strand invasion assay could successfully delineate the kinetics of strand invasion and thermodynamic stability of the DNA:PNA_2 complexes. This simple technique could be useful in studying dsDNA strand invasion by modified oligonucleotides without tedious foot-printing studies. To bring out the true effects of the modified cationic *aep*PNA units more forcefully, bisPNAs bearing neutral linkers such as poly(ethylene glycol) instead of the positively charged Aha-Lys linkers employed here are currently being studied. The study of bisPNAs comprising purines in arm A and pyrimidines in arm B with a view to further understanding PNA_2:DNA triplex formation in the purine motif is also underway.

Experimental Section

The chemicals used were of laboratory or analytical grade and the solvents used were purified according to the literature procedures.[16] All reactions were monitored for completion by TLC and usual workup implies sequential washing of the organic extract with water and brine followed by drying over anhydrous sodium sulfate and evaporation under vacuum. Column chromatography was performed for purification of compounds on silica gel. TLCs were carried out on precoated silica gel GF_{254} aluminum sheets. TLCs were performed with dichloromethane−methanol or petroleum ether−ethyl acetate solvent systems for most compounds. Free acids were chromatographed by TLC, using a solvent system of 2-propanol: acetic acid:water in the proportion 9:1:1. The compounds were visualized with UV light and/or by spraying with ninhydrin reagent after Boc-deprotection (exposing to HCl vapors) and heating. The DNA oligomers were synthesized on CPG solid support by β-cyanoethyl phosphoramidite chemistry followed by ammonia treatment[17] and their purities checked by HPLC prior to use. *aeg*PNA monomers were synthesized according to literature procedures.[13]

Ethyl *N*-(Boc-aminoethyl)-*N*-(chloroacetyl)-glycinate (1).[13] The ethyl *N*-(2-Boc-aminoethyl)-glycinate (4.0 g, 14 mmol) was taken in 10% aqueous Na_2CO_3 (75 mL) and dioxane (60 mL). Chloroacetyl chloride (6.5 mL, 0.75 mmol) was added in two portions with vigorous stirring. The reaction was complete within 5 min after which the reaction mixture was brought to pH 8.0 by addition of 10% aqueous Na_2CO_3 and concentrated to remove the dioxane. The product was extracted from the aqueous layer with dichloromethane and was purified by column chromatography to obtain the ethyl *N*-(Boc-aminoethyl)-*N*-(chloroacetyl)-glycinate **1** as a colorless oil in good yield (4.2 g, 80%).

^{1}H NMR ($CDCl_3$) δ 5.45 (br s, 1H), 4.21 (q, 2H, $J = 7.2$ Hz), 4.14 (s, 2H), 4.00 (s, 2H), 3.53 (t, 2H, $J = 5.7$ Hz), 3.28 (q, 2H, $J = 5.7$ Hz), 1.46 (s, 9H), 1.23 (t, 3H, $J = 7.2$ Hz).

***N*-(Boc-aminoethylglycyl)-(N^2-isobutyryl-*N*7-guanine)-ethyl ester (2a).** A mixture of N^2-isobutyrylguanine (0.6 g,

(15) Demidov, V. V.; Yavnilovich, M. V.; Belotserkovskii, B. P.; Frank-Kamenetskii, M. D.; Nielsen, P. E. *Proc. Natl. Acad. Sci. U.S.A.* **1995**, *92*, 2637.

(16) Perrin, D. D.; Amarego, W. L. F. In *Purification of Laboratory Chemicals*, 3rd ed.; Pergamon Press: New York, 1989.

(17) Barawkar, D. A.; Rajeev, K. G.; Kumar, V. A.; Ganesh, K. N. *Nucleic Acids Res.* **1996**, *24*, 1229.

3.1 mmol), K_2CO_3 (0.43 g, 3.1 mmol), and ethyl *N*-(Boc-aminoethyl)-*N*-(chloroacetyl)-glycinate **1** (0.5 g, 3.1 mmol) was stirred in dry DMF at room temperature overnight. The reaction mixture was filtered and the filtrate evaporated under reduced pressure. The resulting residue was purified by column chromatography to obtain the *N*-(Boc-aminoethylglycyl)-(N^2-isobutyryl-*N*7-guanine) ethyl ester **2a** in 50% yield (0.39 g).

^{1}H NMR ($CDCl_3$) δ 12.25 (s, 1H), 10.13 (s, 1H), 7.90 (s, 1H), 5.85 (m, 1H), 5.33 (major) and 5.13 (minor) (s, 2H), 4.40−4.05 (m, 4H), 3.60 (m, 2H), 3.40 (major) and 3.30 (minor) (m, 2H), 2.55 (m, 1H), 1.45 (minor) and 1.40 (major) (s, 9H), 1.25 (m, 9H); ^{13}C NMR ($CDCl_3$) δ 180.2, 169.4, 167.2, 162.9, 156.4, 153.3, 148.0, 145.2, 112.2, 79.6, 61.5, 48.7, 47.1, 38.7, 35.9, 29.6, 28.4, 18.9, 14.1. M_{calc} = 507.55, M_{obs} = 509.03.

***N*-(Boc-aminoethylglycyl)-(N^2-isobutyryl-*N*7-guanine) (2b).** The *N*-(Boc-aminoethylglycyl)-(N^2-isobutyryl-*N*7-guanine) ethyl ester **2a** (0.39 g, 0.77 mmol) was taken in methanol (2 mL) and aqueous NaOH (2 N, 2 mL) was added. Stirring was continued for 10 min, after which, the excess alkali was neutralized with Dowex H^+ resin, and the filtrate was washed with ethyl acetate before concentration under vacuum to get the product *N*-(Boc-aminoethylglycyl)-(N^2-isobutyryl-*N*7-guanine) **2b** in good yield (0.41 g, 85.5%).

^{1}H NMR (DMSO-d_6) δ 12.15 (s, 1H), 11.60 (s, 1H), 8.10 (s, 1H), 5.40 (major) and 5.20 (minor) (s, 1H), 4.30 (minor) and 4.00 (major) (s, 2H), 3.00 (m, 4H), 2.70 (m, 1H), 2.00 (s, 2H), 1.37 (s, 9H), 1.10 (d, 6H, J = 6.84 Hz). M_{calc} = 479.5, M_{obs} = 481.

1-(*N*-Boc-aminoethyl)-4-(*R*)-*O*-mesyl-2-(*S*)-proline Methyl Ester (3). To a stirred ice-cooled solution of 1-(*N*-Boc-aminoethyl)-4-(*R*)-hydroxy-2-(*S*)-proline methyl ester[5] (1.66 g, 5.9 mmol) in dry pyridine (15 mL) was added dropwise methanesulfonyl chloride (0.55 mL, 7.1 mmol). After 2 h, upon completion of reaction, pyridine was removed under vacuum; the residue was taken in water and extracted with ethyl acetate (5 × 15 mL). The organic layer was dried over sodium sulfate and concentrated to obtain the crude product **3**, which was purified by silica gel column chromatography (0.7 g, 33%).

^{1}H NMR ($CDCl_3$) δ 5.20 (m, 2H), 3.70 (s, 3H), 3.65 (t, 1H, J = 8 Hz), 3.50 (dd, 1H, J = 5 Hz), 3.15 (m, 2H), 3.00 (s, 3H), 2.85 (dd, 1H, J = 3 Hz), 2.75 (m, 2H), 2.35 (m, 2H), 1.45 (s, 9H); ^{13}C NMR ($CDCl_3$) δ 172.7, 155.6, 78.9, 78.6, 65.4, 58.0, 53.1, 51.6, 38.7, 37.9, 36.3, 28.0; $[\alpha]^{25}_{589}$ +26 ° (*c* 2.5, CH_3OH). M_{calc} = 366.43; M_{obs} = 366.

1-(*N*-Boc-aminoethyl)-4-(*S*)-(N^2-isobutyrylguanin-7-yl)-2-(*S*)-proline (4b). A mixture of 1-(*N*-Boc-aminoethyl)-4-(*R*)-*O*-mesyl-2-(*S*)-proline methyl ester **3** (0.15 g, 0.4 mmol), N^2-isobutyrylguanine (0.20 g, 0.9 mmol), and anhydrous potassium carbonate (0.13 g, 0.9 mmol) in dry DMF (2 mL) was kept stirring at 60 °C overnight. The solvent was completely removed under vacuum and the pure product **4a** was obtained (0.06 g, 31%) after column chromatography. The 1-(*N*-Boc-aminoethyl)-4(*S*)-(N^2-isobutyrylguanin-7-yl)-2(*S*)-proline methyl ester **4a** (0.05 g, 0.1 mmol) was taken in methanol (1 mL) and aqueous NaOH (2 N, 1 mL) was added. Stirring was continued for 10 min, after which, excess alkali was neutralized with Dowex H^+ resin, and the filtrate was washed with ethyl acetate before concentration under vacuum to obtain the product 1-(*N*-Boc-aminoethyl)-4(*S*)-(N^2-isobutyryl-guanin-7-yl)-pyrrolidine-2(*S*)-carboxylic acid **4b** in good yield (0.04 g, 82%).

4a: ^{1}H NMR ($CDCl_3$) δ 12.15 (br s, 1H), 9.30 (br s, 1H), 8.40 (s, 1H), 5.65 (m, 1H), 5.20 (m, 1H), 3.75 (s, 3H), 3.30 (m, 4H), 2.80 (m, 5H), 2.20 (m, 1H), 1.45 (s, 9H), 1.20 (d, 6H, J = 6.35 Hz); ^{13}C NMR ($CDCl_3$) δ 179.6, 173.1, 156.4, 156.0, 153.3, 147.5, 142.3, 111.5, 79.2, 64.7, 59.5, 57.9, 53.7, 52.0, 37.6, 35.9, 28.4, 19.0.

4b: ^{1}H NMR (DMSO-d_6) δ 12.22 (br s, 1H), 11.69 (br s, 1H), 8.55 (s, 1H), 6.91 (m, 1H), 5.49 (m, 1H), 3.20 (m, 4H), 2.90 (m, 5H), 2.17 (m, 1H), 1.45 (s, 9H), 1.20 (d, 6H, J = 6.35 Hz); $[\alpha]^{25}_{589}$ −12.88° (*c* 1.32, CH_3OH); M_{calc} = 447.5; M_{obs} = 479.01 and 501.01 [M^+ + H and M^+ + Na^+].

1-(*N*-Boc-aminoethyl)-4-(*S*)-(N^4-benzyloxycarbonyl-cytosin-1-yl)-2-(*S*)-proline Methyl Ester (5a). A mixture of 1-(*N*-Boc-aminoethyl)-4-(*R*)-*O*-mesyl-2-(*S*)-proline methyl ester **3** (0.6 g, 1.6 mmol), N^4-benzyloxycarbonyl-cytosine (1.0 g, 4.1 mmol), anhydrous potassium carbonate (1.1 g, 8.2 mmol), and 18-crown-6 (0.17 g, 0.5 mmol) in anhydrous DMF(6 mL) was stirred under nitrogen atmosphere at 70 °C for 5 h. The solvent was completely removed under vacuum and the residue purified by silica gel column chromatography to obtain **5a** (0.25 g, 30% yield) as the major product. An aqueous solution of NaOH (2 N, 1 mL) was added to a solution of 1-(*N*-Boc-aminoethyl)-4(*S*)-(N^4-benzyloxycarbonylcytosin-1-yl)-2(*S*)-proline methyl ester **5a** and stirred at room temperature for 10 min, when TLC indicated complete hydrolysis of the ester. The reaction was immediately neutralized with Dowex H^+ resin and filtered, and the filtrate was evaporated to obtain the product 1-(*N*-Boc-aminoethyl)-4(*S*)-(N^4-benzyloxycarbonylcytosin-1-yl)-pyrrolidine-2(*S*)-carboxylic acid **5b** (0.58 g, 99.5% yield) as a hygroscopic white solid

5a: ^{1}H NMR ($CDCl_3$) δ 8.45 (d, 1H, J = 6 Hz), 7.40 (s, 5H), 7.25 (d, 1H, J = 6 Hz), 5.35 (t, 1H, J = 6 Hz), 5.20 (s, 3H), 3.75 (s, 3H), 3.20 (br m, 4H), 2.80 (m, 2H), 2.60 (m, 1H), 1.90 (m, 2H), 1.45 (s, 9H); ^{13}C NMR ($CDCl_3$ + CD_3OD) δ 173.7, 162.6, 160.9, 156.5, 146.4, 135.4, 128.9, 128.6, 128.5, 128.1, 125.2, 96.3, 79.6, 67.7, 65.1, 58.3, 54.5, 53.3, 52.2, 39.0, 36.8, 28.3; $[\alpha]^{25}_{589}$ +9.63 ° (*c* 0.003, CH_3OH). M_{calc} = 515.57; M_{obs} = 517.7.

5b: ^{1}H NMR (CD_3OD) δ 8.10 (d, 1H, J = 7.3 Hz), 7.40 (m, 7H), 5.24 (s, 2H), 4.02 (m, 1H), 3.55 (m, 3H), 3.34 (m, 4H), 3.08 (m, 1H), 2.36 (m, 1H), 1.45 (s, 9H); $[\alpha]^{25}_{589}$ −16.07° (*c* 0.28, CH_3OH). M_{calc} = 485.5, M_{obs} = 503.01 [M^+ + NH_4^+].

Synthesis and Cleavage of the PNA Oligomers from the Solid Support. The PNA oligomers were synthesized manually by solid-phase peptide synthesis by using the Boc-protection strategy and employing diisopropylcarbodiimide (DIPCDI) and 1-hydroxybenzotriazole (HOBt) as the coupling agents. The solid support used was Merrifield resin that was derivatized with β-alanine (0.13 mequiv/g of resin) as the spacer amino acid. Synthesis involved repetitive cycles, each comprising (i) deprotection of the N-protecting Boc-group with 50% trifluoroacetic acid (TFA) in CH_2Cl_2, (ii) neutralization of the TFA salt formed with diisopropylethylamine (5% solution in CH_2Cl_2, v/v), and (iii) coupling of the free amine with the free carboxylic acid group of the incoming monomer (3 to 4 equiv) in the presence of DIPCDI and HOBt, in DMF or NMP as the solvent. The deprotection of the *N*-Boc protecting group and the coupling reaction were monitored by Kaiser's test.[18] Since the coupling efficiencies were found to be >98%, capping of the unreacted amino groups was not found necessary.

The PNA oligomers were cleaved from the solid support by using the TFA-trifluoromethanesulfonic acid (TFMSA) method to yield oligomers with free carboxylic acids at their carboxy termini.[19] The resin-bound PNA oligomer (10 mg) was stirred in an ice-bath with thioanisole (20 μL) and 1,2-ethanedithiol (8 μL) for 10 min. TFA (120 μL) was then added and the stirring was continued for another 10 min. TFMSA (16 μL) was added while the reaction was cooled in an ice-bath and stirring was continued for 2 h. The reaction mixture was filtered through a sintered funnel, the residue was washed with TFA (3 × 2 mL), and the combined filtrate and washings were evaporated under vacuum. The residual pellet was redissolved in methanol (~0.1 mL) and reprecipitated by adding ether to obtain the crude PNA oligomer. This was purified by gel filtration over Sephadex G25. The purity of the PNA oligomer was checked by RP HPLC on a C18 column and found to be >90%.

MALDI-TOF: **PNA 6**, M_{obs} = 4499.75, M_{calc} = 4495.64; **PNA 7**, M_{obs} = 4580.88, M_{calc} = 4575.69; **PNA 8**, M_{obs} = 4493, M_{calc} = 4491.69; **PNA 9**, $[M]_{obs}$ = 4593 [M^+ + Na^+], M_{calc} = 4571.74.

(18) Kaiser, E.; Colescott, R. L.; Bossinger, C. D.; Cook, P. I. *Anal. Biochem.* **1970**, *34*, 595.

(19) Fields, G. B.; Fields, C. G. *J. Am. Chem. Soc.* **1991**, *113*, 4202.

UV-Melting. The concentration of the PNA oligomers was calculated on the basis of the absorption at 260 nm, assuming the molar extinction coefficients of the nucleobases to be as in DNA, i.e., T, 8.8 $cm^2/\mu mol$; C, 7.3 $cm^2/\mu mol$; G, 11.7 $cm^2/\mu mol$; and A, 15.4 $cm^2/\mu mol$. The hairpin bisPNA oligomer (**6**−**9**) and the relevant complementary DNA oligonucleotide (**10**/**11**) were mixed together in a 1:1 molar ratio in 0.01 M sodium phosphate buffer, pH 5.8 or 7.4, to get a final strand concentration of 1 μM. The samples were annealed by heating them at 85 °C for 1−2 min, followed by slow cooling to room temperature, kept at room temperature for ∼30 min, and then refrigerated overnight. The samples were heated at a rate of 0.5 °C rise per minute and the absorbance at 260 nm was recorded every minute. The percent hyperchromicity at 260 nm was plotted as a function of temperature and the melting temperature was deduced from the peak in the first derivative plots.

Fluorescence Strand Invasion Assay. The strand invasion studies were performed in 5 mM sodium phosphate buffer, pH 5.8 or 7.4, at 20 °C. The DNA duplex **10**:**12** (2 μM) was annealed by the procedure described above and saturated with ethidium bromide (∼1 μM) prior to addition of the PNA strand (**6**−**9**, 20 μM). The fluorescence intensity at 590 nm (λ_{max}) was recorded every 10 min and was plotted as a function of time.

Acknowledgment. M.D. thanks CSIR for a research fellowship. V.A.K. thanks the Department of Science & Technology and K.N.G. and V.A.K. thank the Department of Biotechnology, New Delhi, for financial support.

Supporting Information Available: HPLC profiles of PNA oligomers **6**, **7**, **8**, and **9**; mass spectra of **4b** and **5a**, **2a** and **2b**, **4b** and **5b**, PNAs **6** and **7**, and PNAs **8** and **9**; UV melting plot of the first derivative of the percent hyperchromicity vs temperature profiles of complexes of PNA **6**−**9** with DNA **10**. This material is available free of charge via the Internet at http://pubs.acs.org.

JO034048H